Bioinspiration & Biomimetics

PAPER

Transportation networks inspired by leaf venation algorithms

To cite this article: Fernando Patino-Ramirez and Chloe Arson 2020 *Bioinspir. Biomim.* **15** 036012

Bioinspiration & Biomimetics

PAPER

Transportation networks inspired by leaf venation algorithms

RECEIVED
14 November 2019

REVISED
6 February 2020

ACCEPTED FOR PUBLICATION
12 February 2020

PUBLISHED
25 March 2020

Fernando Patino-Ramirez and Chloe Arson

School of Civil and Environmental Engineering, Georgia Institute of Technology, Atlanta, GA, United States of America

E-mail: fp@gatech.edu

Keywords: optimization, leaf venation, transport efficiency, pareto, graph theory

Abstract

Biological systems have adapted to environmental constraints and limited resource availability. In the present study, we evaluate the algorithm underlying leaf venation (LV) deployment using graph theory. We compare the traffic balance, travel and cost efficiency of simply-connected LV networks to those of the fan tree and of the spanning tree. We use a Pareto front to show that the total length of leaf venations (LVs) is close to optimal. Then we apply the LV algorithm to design transportation networks in the city of Atlanta. Results show that leaf-inspired models can perform similarly or better than computer-intensive optimization algorithms in terms of network cost and service performance, which could facilitate the design of engineering transportation networks.

1. Introduction

The seemingly simple problem of connecting a central node to a set of spatially scattered points is common to many natural and artificial systems of all scales and levels of complexity. Despite the differences in the mechanisms that drive network deployment, optimality is always sought as the maximum of objective functions under environmental constraints. Performance metrics are defined *a priori* by the modeler. A complex system can be optimized locally or globally, and optima may vary over time due to environmental constraints or internal changes such as ageing, growth and demand and supply. Complex optimization problems have been addressed by nature for millions of years by means of evolution; external stimuli trigger adaptation of organisms (and their organs) to their environment (constraints) and the competition for resources results in increasingly efficient organs, organisms, communities and ecosystems over subsequent generations [1–4].

In closed environments with a limited availability of resources, biological networks constantly adapt to improve their efficiency, robustness or flexibility. Principles of thermodynamics impose some trade-offs: increased efficiency towards a specific function decreases the performance of the network in some other manner. In the case of fully connected graphs, minimization of the total network length results in a simply connected graph, having exactly one unique path between every pair of nodes [5]. Conversely, dynamic environments promote the development of robust and resilient networks, capable of overcoming accidents and errors and that have a better evolvability, at the expense of an increased network cost [6–10].

Organs and tissues develop strategies to optimize flow, energy, cost, connectivity and any other characteristic pertinent to their function. For instance, circulatory vessels are shaped to ensure efficiency and resilience [11]; neural arbors deploy with minimum distance between cell bodies and synaptic partners and minimum network cost [12]; plants optimize flow from roots to leaves while minimizing the total energy cost of their growth [13]; root systems follow high hydraulic gradients [3, 4, 14] and uptake water as they grow, which makes the soil-root dynamics highly coupled and non-linear [15–17]. Remarkable optimization strategies were also noted in relatively low complexity organisms, including fungus [18] and slime mold, a unicellular organism capable of achieving continuous optimization of its foraging path [19, 20]. Computational algorithms inspired by slime molds were used to aid solving NP-complete problems, such as finding Steiner trees (STs) [19, 21], and to assist the design of transportation networks [22–24]. Communities have been studied extensively through ant colonies, which minimize the local cost of their networks [25] to the expense of reduced robustness [26]. Related research focuses on colony organization [27, 28], robustness versus efficiency [29] and computational

optimization algorithms [30]. Other animals exhibit intrinsic optimization strategies [31, 32] in their travel and exploration dynamics.

Bio inspiration has been adopted in many disciplines as a vector of innovation. For instance, doctors practice surgeries with a mosquito-inspired needle [33]; cod glycoproteins are used in the industry for their antifreeze properties [32]; wind turbines were optimized by taking inspiration from the flippers of humpback whales [34] and mussels inspired the fabrication of novel adhesive compounds [35]. Engineering and natural networks present similarities both in their global and local optimization objectives. For instance, water networks were designed by solving an NP-complete problem using particle-swarm optimization, with a bird-flock inspired algorithm [36]. Internet networks were optimized with an algorithm inspired by slime molds [37]. Bus routes were calculated based on ants behavior [38].

In this study, we evaluate a leaf venation (LV) algorithm for designing bio-inspired infrastructure networks. In section 2, we describe an algorithm that models the mechanisms that drive LV deployment and we present two reference algorithms for benchmarking. In section 3, we compare the LV algorithm to the two reference models by means of a set of topological indexes and a Pareto optimality front. In section 4, we apply the LV algorithm to design a transportation network in the metropolitan area of the city of Atlanta (GA) and to expand the current metropolitan network towards an adjacent suburban county. Section 5 presents our conclusions regarding the potential of using LV algorithms for infrastructure design.

2. Network algorithms

LVs connect the stem to points distributed on the blade of a leaf with minimum length to transport fluids under environmental constraints. Similarly, transportation networks connect areas with high population or high economic activity and are designed to minimize cost and maximize efficiency during construction and service life. Based on this analogy, we propose to apply an LV algorithm to design a transport infrastructure network under the following assumptions: (i) The existence of a single source/sink point connected to an arbitrary number of attraction/service points; (ii) The absence of healing mechanisms that can overcome possible disconnections; (iii) The possibility of discretizing the domain into nodes that need to be connected (called attraction points from now on). In this section, we present LVs as simply connected networks embedded in a homogeneous space at steady state and we compare the performance of the LV algorithm to that of two benchmark network algorithms.

2.1. Leaf venation (LV)

Plant leaves grow a vascular system of interconnected veins, which ensure evapotranspiration and mechanical stability [4, 39]. LV systems form hierarchical networks, usually starting with a main single vein that grows from the petiole, followed by secondary branches that start from the main vein, and are connected at the same time to smaller veins. The latter, called tertiary veins, create paths that connect every single stoma to primary and secondary veins and therefore permit flow from/to the petiole to the whole leaf blade [40]. Additionally, tertiary veins form loops in the network, adding redundancy to the system so that in case a vein is cut, flow paths still exist to reach the entirety of the leaf blade; the existence of loops in the network increases its overall cost [41]. Here, we study cost minimization and thus focus on primary and secondary veins. We do not study the mechanical stability of the leaf and focus on the mass transport function of the LV.

Vein development [42] influences the shape and growth of the leaves [43, 44]. Leaf blade shapes are either simple (with a single unit) or compound (with two or more leaflets). Simple leaves can be entire, if they have a smooth or slightly toothed edge, or lobed, if they have significant indentations that make the contour highly non-convex [44]. Marginal growth characterizes leaves that develop outside of the current blade contour whereas diffuse growth refers to blades that stretch themselves to increase area [42]. In our study, we focus on simple, entire leaves that experience no growth; thus, we study the case of a relatively unconstrained geometric domain that grows outwards (no stretching of existing veins). This scenario is congruent with transportation infrastructure networks, which are constructed progressively, extending from the previous step of the network.

The most accepted algorithm for modelling vein patterns formation is based on the canalization hypothesis [45], which states that the growth and branching of new veins are controlled by the spatial distribution of a signal distributed along the leaf blade. This signal is in large part attributed to a growth hormone called auxin. Physical evidence shows that auxin sources can be viewed as attraction points discretely distributed throughout the blade [46] and numerical LV algorithms based on that assumption were validated against biological experiments [44]. The diameter of the veins obeys Murrays law, a power law with exponents that depend on plant species [47].

In the present study, we adopt the algorithm proposed by Runions [44]. The algorithm is described in figure 1. In this implementation, the domain and auxin points (attraction points) are fixed at the start of the algorithm, and no new auxin point is added over time. Rectangular domains were used, and the kill distance was set as 0.5% of the largest dimension of the domain. After the LV architecture is obtained, it is transformed into an undirected graph, preserving the source, branching and attraction points and their connectivity, therefore making the edges between nodes straight lines.

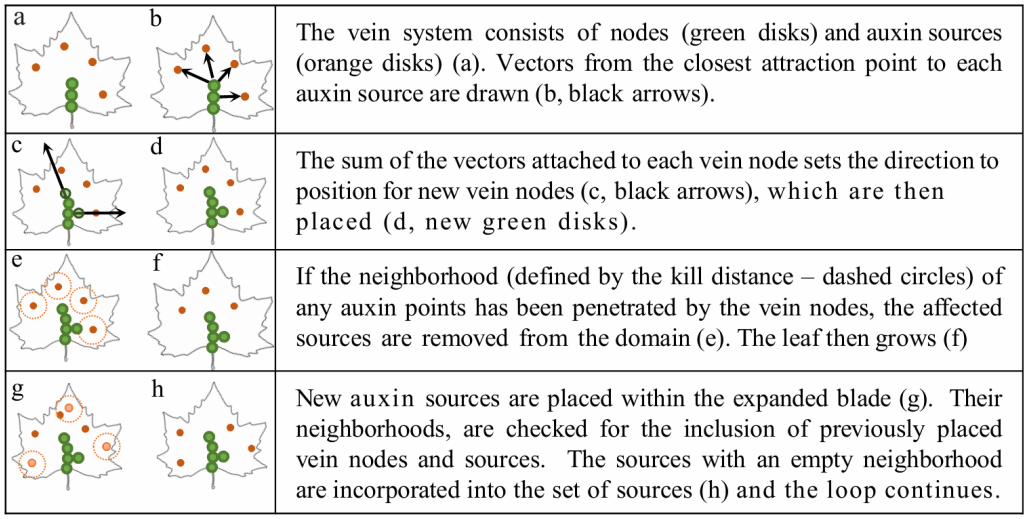

Figure 1. LV pseudo-algorithm, after Runions [44].

2.2. Benchmark networks

In the following, let Tl be the network that minimizes each objective function. We benchmark the LV algorithm against a local optimization algorithm (fan tree), for which T_l is defined as the sum of the minimum source-attraction point distances, and a global optimization algorithm (ST), for which T_l is the minimum total length of the edges in the network. The fan and STs are constructed to connect a given set of points regardless of whether they are source or attraction points. The fan tree and the ST results are then used to construct a Pareto optimality front [48].

2.2.1. Fan network (FN)

The total length of a network that minimizes each travel distance from the source node to an attraction point can be expressed as:

$$T_l = \sum_{i}^{n} d_i$$

where d_i represents the distance along the edges from the source point to the ith attraction point, $i \in \{1, \ldots, n\}$.

The network that minimizes T_l is a fan network (FN), i.e. a collection of straight lines from the source to each sink. The FN represents a local optimum for each travel distance from the source. The nodes of the FN are only the source and the attraction point, i.e. there is no branching node.

2.2.2. Steiner tree (ST)

A ST is a network that connects a set of points with the minimum total network length [49–51]. Additional branching nodes (called Steiner points) can be introduced in the system. The global optimization criterion for STs can be expressed as:

$$T_l = \min\left(\sum_{i}^{m} e_i\right)$$

where e_i represents the length of edge $i \in \{1, \ldots, m\}$. Note that m designates the number of node-to-node segments in the ST, which comprises nodes other than the source or the attraction points (Steiner points).

The basic Euclidean ST problem is in an unconstrained domain without obstacles [51]. Subsequent advanced algorithms that proposed to include obstacles and other geometries [54–57] are NP-complete problems, i.e. the running time of the algorithm grows exponentially with the number of nodes [52, 53]. In order to circumvent the exponential increase of the runtime with the number of nodes, heuristics and alternative algorithms have been developed to approximate the solution and/or obtain an initial guess of the solution; some of these approaches have taken inspiration from bio-inspired systems such as slime mold growth algorithms [19, 21]. In the current implementation, we follow the algorithm proposed by Fonseca and collaborators [58] to find the STs, which are then transformed into undirected graphs for analysis.

2.3. Pareto efficiency

We analyze the optimality of networks to satisfy: (i) A local criterion, to minimize the sum of the travel distances from the source/sink point to each attraction point along the edges of the network; (ii) A global criterion, to minimize the total network length. The Pareto optimality front [48] is an optimality line that indicates the smallest sum of individual distances that can be obtained for a given total network length.

In order to generate the Pareto front, we create solutions that follow a joint optimization objective, which is a linear combination between the two optimization criteria evaluated. The combination of the objectives is controlled by a parameter $0 \leqslant \alpha \leqslant 1$; when $\alpha = 0$, the objective reduces to the local criterion (FN), while when $\alpha = 1$, the objective reduces to the global criterion (ST).

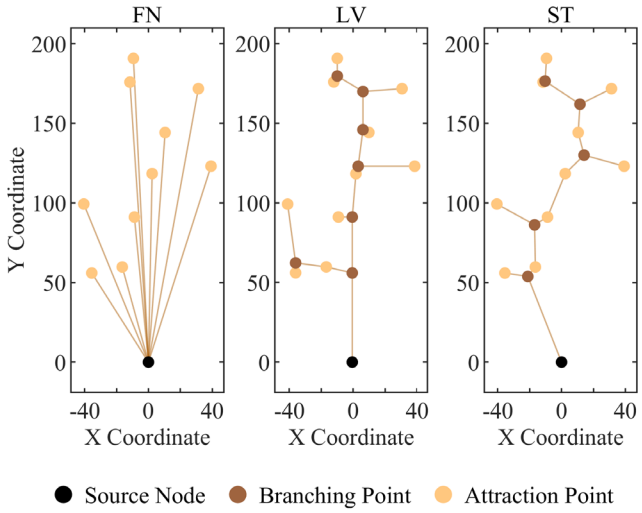

Figure 2. Example network topologies: FN, LV and ST. Results for a set of ten random attraction points.

To do so, we use the available plant-inspired greedy algorithm developed and implemented by Conn and collaborators [13], which constructs near-optimal architectures as shown in [12, 13, 59]. The algorithm starts from a stem protruding from the source node towards the centroid of the attraction points. From there, new branching points (and branches) are iteratively tested, choosing the branch that minimally increases the value of the objective (a function of α).

A network is considered Pareto optimal for the criteria tested if it lies along the Pareto front. We hypothesize that LV networks optimize one of the optimization criteria tested or a combination of both (along the Pareto front). Nevertheless, LVs are not only optimized for travel distances and cost, but also for other criteria not studied here [13, 48] related to mechanical stability, genetics, heat transfer among others.

3. Evaluation of optimality

3.1. Arbitrary networks evaluation

In order to analyze the underlying optimization mechanisms of leaf-inspired algorithms, we generated networks that connect a source to randomly distributed sets of attraction points in a 2D rectangular domain. The source node (petiole of the leaf) was placed at the bottom center of the domain (coordinates [0,0]). We tested 50 replicates of 10 attraction points (auxin points), and 50 replicates of 15 attraction points. The coordinates of the attraction points were uniformly distributed, in the range [−50 50] along the *X*-axis, and in the range [30 200] along the *Y*-axis. The *Y* range was set to start from 30, to create a distance between the source node ([0,0]) and the rest of the nodes, and therefore, enhance the tree-like structure of the resulting networks. The networks obtained are characterized as undirected graphs, in which the nodes correspond to the input points plus the set of branching points generated by each one of the algorithms. Figure 2 shows an example of the obtained networks for a set of ten attraction points.

3.2. Pareto optimality

For each of the 100 sets of attraction points (called replicates in the following), we generate the LV, the FN, and the ST. For each network, the sum of individual travel distances from the source to each attraction point along the edges of the graph (local index) and the total network length (global index) are calculated. To aid visualization, we normalize the indexes according to the optimal bounds. The FN exhibits the lowest sum of individual travel distances and therefore its local index is mapped 0 and its global index set as 1; conversely, the ST exhibits the lowest total network length and therefore its global index is mapped to 0 and its local index set to 1. Then, the indexes of the LV are mapped based on the global and local bounds. Figure 3 shows the results. The shaded region encloses the Pareto fronts of all the replicates, which are also normalized. Contiguous boxplots show the variability of the sum of the individual travel distances and of the total network length among the 100 LV networks.

The total network length of the LV networks is close to the theoretical minimum (median value of 0.04) with a small variability (maximum value 0.11 and minimum value of 0.01). On the other hand, the sum of travel distances from the source shows high variability, ranging from 0.51 to 2.31 with a median of 1.27. This result suggests that the LV algorithm seeks to minimize the global network length but does not optimize the sum of individual distances to the source.

3.3. Service life performance

The optimization criteria used to plot the Pareto front are related to the initial design of the network. In addition to cost, travel path efficiency and load (traffic) balance are also important performance metrics of a transport network during its service

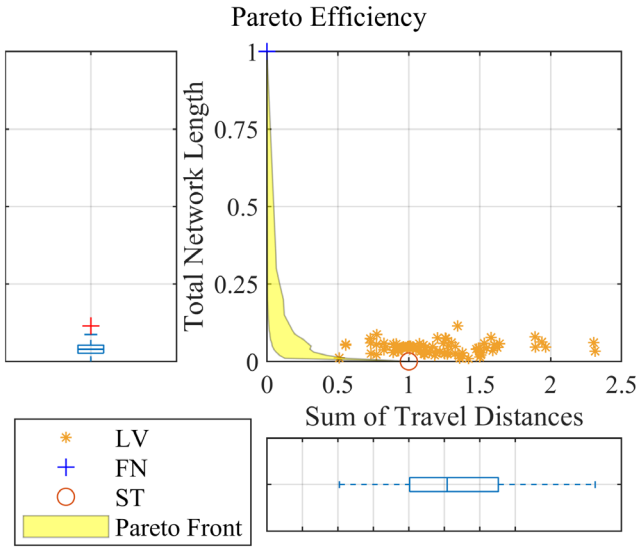

Figure 3. Normalized Pareto front, for 100 replicates of randomly distributed attraction points. Scattered dots correspond to the results obtained with the LV algorithm. Adjacent boxplots illustrate the variability of the local and global network indexes.

life. In the following section we study the service life performance assuming that the capacity (proportional to the width of the edges) is homogeneous and fixed for all the edges of the graphs.

3.3.1. Load balance: edge congestion

Load or traffic balance is a common measure of service performance that has attracted a lot of attention in the field of graphs theory [5, 60]. Depending on the context, the interpretation of load distribution has different meanings:

Congestion: if the capacity or width of the nodes or edges of the network are fixed and/or homogeneous, the system may suffer from bottleneck congestion, where the transport efficiency is controlled by the most congested link; therefore a uniform load distribution is optimal—like in parallel computing [61].

Centrality: if the capacity of the elements of the network is not a limitation, the distribution of the traffic load is a measure of the node/edge importance inside the network; therefore an irregular distribution of load is desired in order to classify or identify components in the network—like in social media networks [62, 63].

A common metric to find the load distribution in a graph is the node betweenness centrality [62]; it is defined as the number of times a given node is part of the shortest path between two other nodes of the network, normalized by the number of nodes in the graph. In the current analysis, we use a slightly modified metric of load balance: we compute the load in the edges rather than the nodes, and we consider the traffic between every pairwise combination from the set of source and attraction nodes (excluding the branching/Steiner points). That way, the load balance only stems from the set of nodes that is common to all networks. For each of the algorithms evaluated in the benchmark, we plot the mean value of load balance and the interquartile range (IQR), a measure of dispersion that corresponds to the difference between the 25th and 75th percentiles of the data. Results are shown in figure 4.

For the current assumption of homogeneous and fixed edge capacity, we find that the LV and ST solutions have similar values of edge congestion, with median mean values of 0.31 and 0.37, respectively. Nevertheless, the traffic load is more evenly distributed in LVs than in STs: the IQR medians are 0.24 and 0.33 for LV and ST, respectively. On the other hand, the FNs outperform the STs and LVs, with a smaller median mean load (0.25) and a perfect load balance (IQR = 0)—since all the edges are used the same number of times.

These results suggest that longer networks are more likely to balance traffic, since resources are not limited. But as the total network length decreases, the load is concentrated in certain edges, causing increased edge congestion.

3.3.2. Travel path efficiency

Besides load balance, the efficiency of traffic or flow during service life depends on the travel distance between pairs of nodes. We define travel path efficiency as the ratio between the travel distance between two nodes in a network and their Euclidean distance in the 2D domain.

We first evaluate the paths from the source node to each attraction point, as shown in figure 5. We then analyze the path efficiency between every pair of nodes (excluding branching points), as shown in figure 6.

By definition, the FN algorithm exhibits perfect path efficiency from the source, where every path has an efficiency of 1 (no dispersion). The LV algorithm outperforms ST both in terms of mean value and dispersion: LV median mean efficiency and IQR are 1.15 and 0.12, against 1.27 and 0.21 for the STs. Path efficiency among pairs of nodes cannot be optimal for

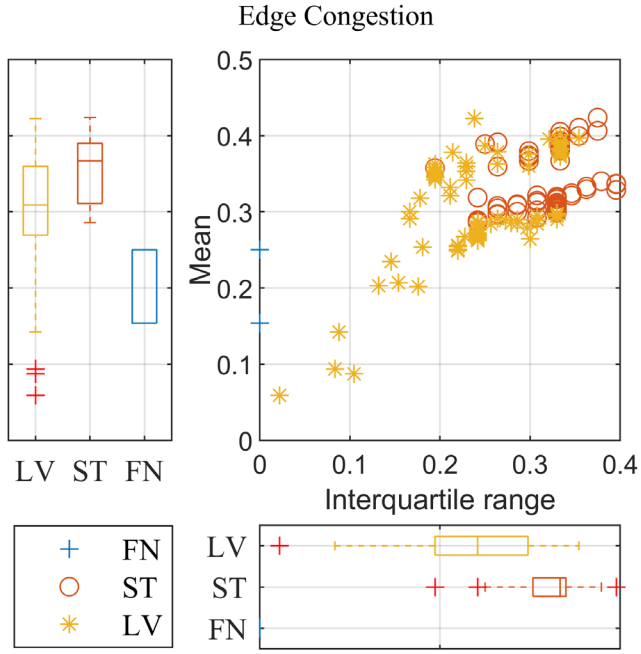

Figure 4. Edge congestion distribution. Vertical values show the mean edge congestion for the different networks while the horizontal axis shows its variability, in terms of the interquartile range.

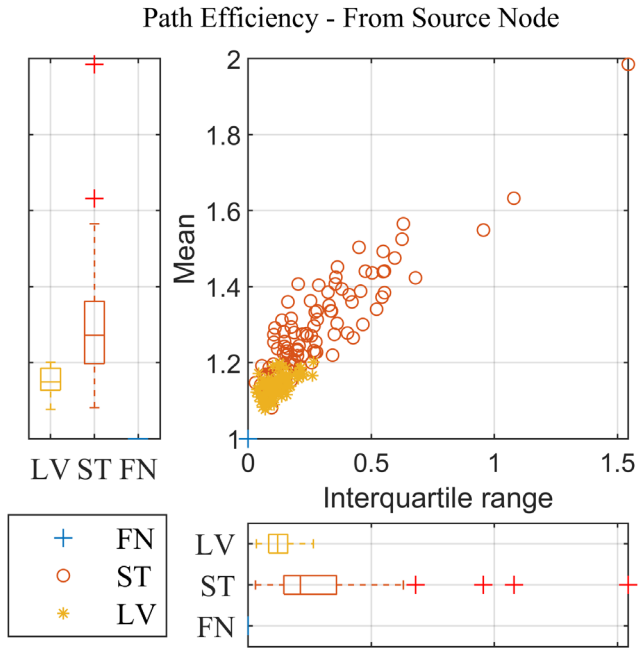

Figure 5. Travel path efficiency, paths from the source node to the attraction points.

simply connected graphs because edges are used in multiple paths. Not surprisingly, FNs have the lowest performance in this index, with median mean values from 3.38 to 10.34, because the load has to travel through the source to reach the destination node. The ST algorithm outperforms LV: the median mean value is 1.59 for LVs and 1.34 for STs, and the median IQR is 0.59 for LVs and 0.29 for STs.

4. Proof of concept: transportation networks in Atlanta, GA

Urban transportation networks are designed at minimum length (or cost) for optimal path efficiency and traffic balance, under land use and budget constraints. Here, we compare the performance of the LV algorithm to that of the ST for designing

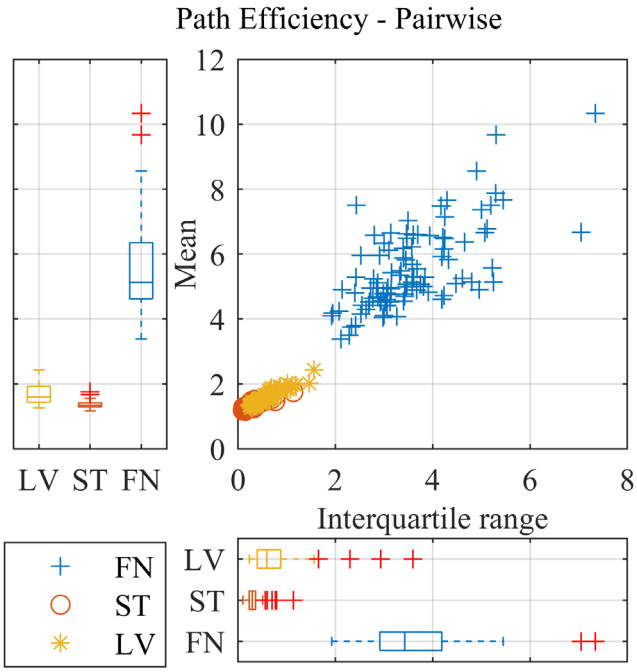

Figure 6. Travel path efficiency, paths joining pairs of attraction points.

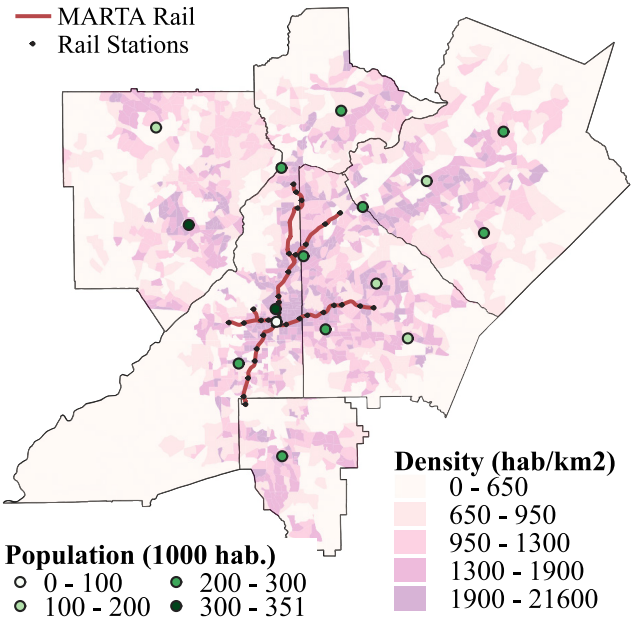

Figure 7. Density of population of the metropolitan area of the city of Atlanta (shaded background) and the corresponding fifteen population centroids (red dots). MARTA railways network shown in red solid lines.

transportation networks in the city of Atlanta (GA), for which the population density map is available from the census of 2010 [60].

4.1. Atlanta metropolitan area

We start by studying the five most populated counties of the metropolitan area of the city (Fulton, Gwinnett, Cobb, DeKalb and Clayton), and we compare LV and ST networks with a uniform-fixed edge capacity. The metropolitan area of Atlanta spans radially from an economic and geographic center. The natural center of the city (and the most densely populated area) is downtown, which also concentrates a large amount of venues of interest including auditoriums, stadiums, touristic sites and business and commercial operations. Therefore, we set the source node of the network as the location of the actual hub on the railway lines: Five Points station in the heart of downtown.

The attractions points are population centroids. We use a weighted k-means algorithm [61] to calculate the position of fifteen attraction points. Each attraction point is the weighted centroid of the region that

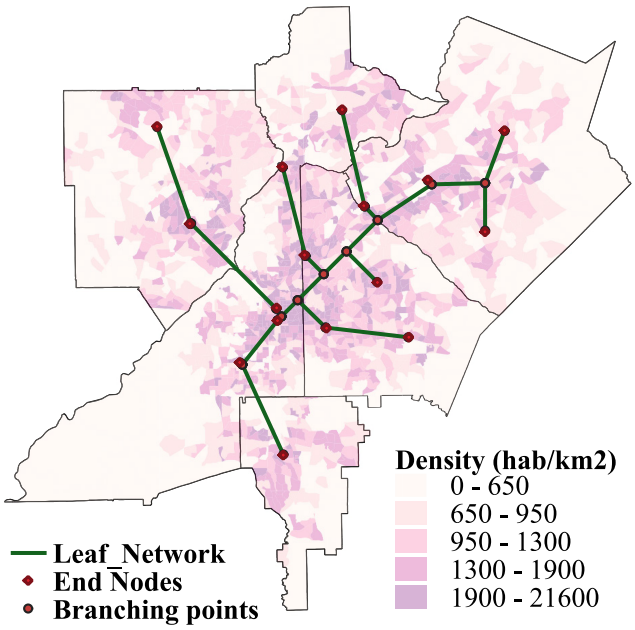

Figure 8. LV network connecting the 15 discrete density of population centroids in Metro Atlanta.

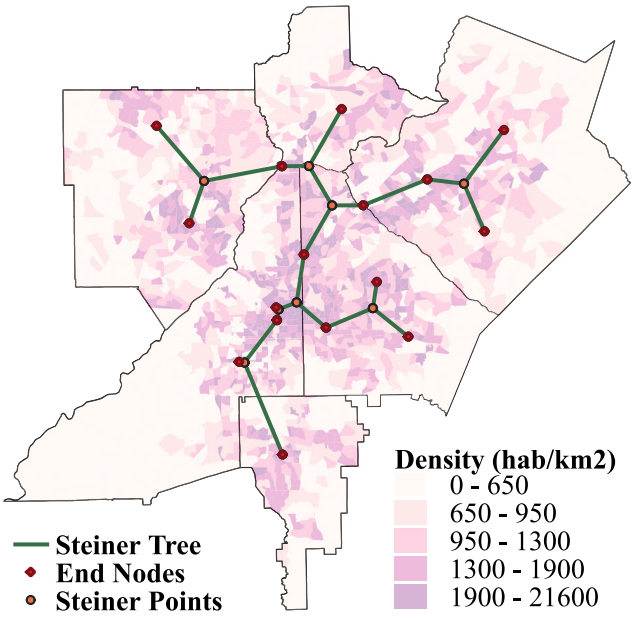

Figure 9. ST, resulting network connecting the 15 discrete density of population centroids in Metro Atlanta.

contains the population that lives closer to that attraction point than to any other attraction point. Figure 7 shows the distribution of the density of population by census tract, shown as shaded regions, and the attraction points. For context, we also show the actual metro system of the city: the MARTA railway. The LV and ST networks are shown in figures 8 and 9, respectively. The FN was computed as well to calculate the Pareto optimality line.

4.1.1. Pareto optimality

Following the same strategy as that described in section 3.2, we build the Pareto front that spans between the FN and the ST as shown in figure 10.

Results before normalization show that the FN and LV networks are, respectively, 106.7% and 10.53% longer than the ST. The sum of distances from the source is 14.86% larger in the LV than in the FN and 25.10% larger in the ST than in the FN. The LV thus

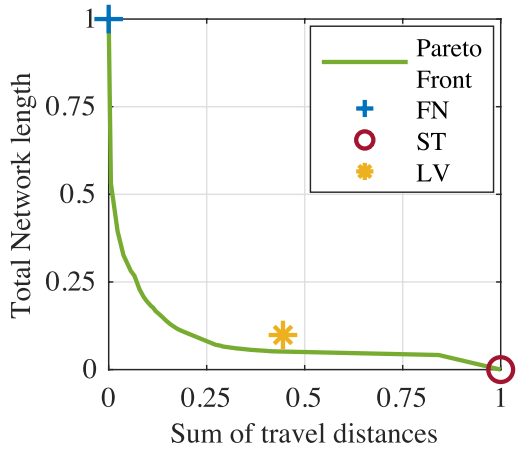

Figure 10. Pareto front and LV network for the transportation system built in the metropolitan area of Atlanta.

outperforms the ST for individual travel distances. The LV algorithm proves to be close to optimal, at a small distance from the Pareto front, with a high performance with respect to individual travel distances at the expense of network slightly longer than optimal.

4.1.2. Load balance and travel path efficiency

We measure the load balance following the method explained in section 3.2.1, except that the travel path between every pair of nodes is weighted according to the population associated to the nodes connected. Every edge that is a part of a travel path is assigned half of the total population represented by the two nodes that it connects. The total assigned population of an edge is the sum of the population assigned to that edge for all the paths that the edge is part of. The source node is assigned a weight of zero. Once the total congestion is calculated, the values are normalized by the total population. Figure 11 shows the load balance of the networks. The LV network shows a lower mean and interquartile range compared to the ST, suggesting that the edge load is slightly more homogeneous in the LV.

The travel path efficiency is evaluated as explained in section 3.2.2. Figure 12 shows the boxplots with the distribution of the path efficiency of the networks for both conditions. Additionally, table 1 summarizes the mean and IQR values. The distribution of the path efficiency from the source shows a small difference between the networks, with the LV exhibiting a better travel efficiency than the ST. On the other hand, the distributions of path ratio from all the centroids (attraction points and source) are similar for both networks, the LV performing slightly better than the ST.

4.1.3. Population served: buffer method

We now assess the networks in terms of the population that they serve. We use the Geographic Information System (GIS) to calculate the total number of inhabitants (based on census tracts) that are within a distance of 2 km (walking distance) from the networks. The area bounded by the offset distance from the network is known as the buffer region. The buffer method is commonly used to evaluate transportation and service networks [64, 65].

Figure 13 presents the total population inside the buffer, the buffer area and the networks length. The three buffer variables exhibit similar trends: the FN reaches the largest population, covers the largest area and has the highest network length. The LV is in second place and the ST is last. Interestingly, the values for the LV metrics are consistently about 10% higher than the ones of the ST. Figure 14 shows similar indexes, this time normalized by network length or buffer area. The population served per unit length shows that the most efficient networks are the ST (5317 hab km^{-1}) followed closely by the LV (5248 hab km^{-1}—1.3% difference); the FN reached 3687 hab km^{-1}—30.7% difference. The area of the domain served by unit length of network is 4.03 km^2 m^{-1} for the ST, 3.99 km^2 m^{-1} for the LV (1% difference) and 2.82 km^2 m^{-1} for the FN (30.1% difference).

Lastly, the population density inside the buffer areas was very uniform along the networks, with an average of 1313 hab km^{-2} and less than 1% difference among networks. These results suggest that even though the resource concentration of the domain is the same for all the networks, the ST and the LV cover it more efficiently, both in term of area covered and population served. The LV reached 10% more area and population than the ST, at the price of an increase in network length of 10%.

4.2. Gwinnett county

Gwinnett county is the second most populated county of the metropolitan area of Atlanta and is still not served by any railway to this date. We model the expansion of the MARTA railway network with the LV and the ST algorithms. By contrast with the modelling exercise presented for the whole Atlanta metropolitan area, the network expansion spans from a source node that may have a considerable effect on the overall urban network. Additionally, the edge capacity is not fixed or uniform.

We first discretize the population map of Gwinnett county by calculating the position of five weighted population centroids with a weighted k-means algorithm. The source node is represented by the current MARTA station that is the closest to Gwinnett county. The resulting LV and ST networks are shown in figures 15 and 16, respectively.

The total length of the LV is 6.1% higher than that of the ST (LV: 50.05 km; ST: 47.18 km). Regarding the population served, the LV reaches 10% more inhabitants than the ST (LV: 254 594 hab; ST: 231 496 hab). The area covered by the LV is 4.23% higher than the ST. Table 2 summarizes the normalized indexes of population/area. We observe that even though both networks cover a similar area per unit length of network, the LV is more efficient, both in terms of population per unit

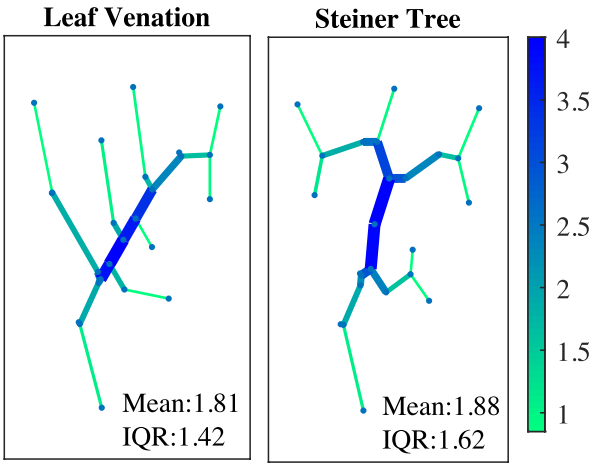

Figure 11. Load balance as edge congestion. Edge thickness and color are proportional to edge congestion.

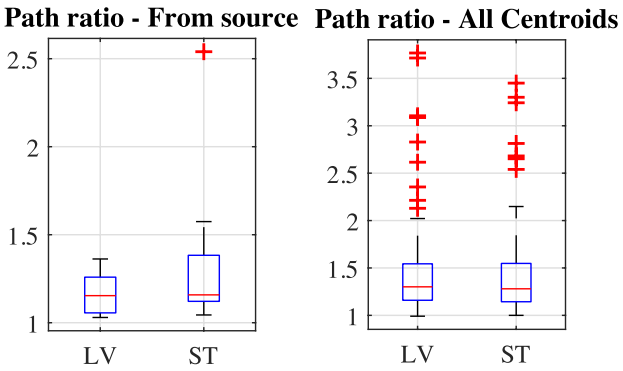

Figure 12. Path efficiency for the LV and ST networks in the metropolitan area of Atlanta.

Table 1. Path efficiency distribution, networks in metropolitan area of Atlanta.

	From Source		All Centroids	
Path Ratio	Mean	IQR	Mean	IQR
LV	1.16	0.20	1.43	0.38
ST	1.32	0.26	1.45	0.40

length of network and in terms of total population reached. This is because the LV passes through regions with an increased density of population.

By contrast with the cases simulated in sections 3.2.1 and 4.1.2, in which networks have edges of homogeneous capacity, we now consider that edge capacity is a design variable, and that, according to section 3.2.1, edge capacity should be proportional to its traffic load. We assume that the cost of each edge of the network is proportional to the product of its length by the load going through it (e.g. number of lanes multiplied by the length of the road). The total cost of the network is calculated as:

$$\text{cost} = \sum_{i}^{n_E} C_i \cdot L_i$$

where C_i is the traffic through the edge (i.e. the edge load, calculated as explained in section 4.1.2), L_i the segment length and n_E is the number of network edges. We study the change in traffic distribution and network cost as a function of the weight (population) of the source node (W_0). The influence of the source node on the network is proportional to its weight. We vary the weight of the source node from zero (similar to section 4.1.2) to a maximum value corresponding to the population of the four adjacent counties to Gwinnett. The population of the adjacent counties is 2749 889, about 3.1 times the population of Gwinnett County (889 954). Figure 17 shows the traffic distribution for three different W_0 values: zero, Gwinnet's population, and the population of the adjacent counties. Networks are relatively independent from the rest of the railway system for homogeneous traffic loads, while for a concentrated load, the traffic is routed to a main vein in the neighborhood of the source node.

Figure 18 shows the evolution of the total network cost and of the cost per unit length of network, as a function of the source node weight (W_0) normalized by the population of the county. Results show that, for networks with low dependency on a source node,

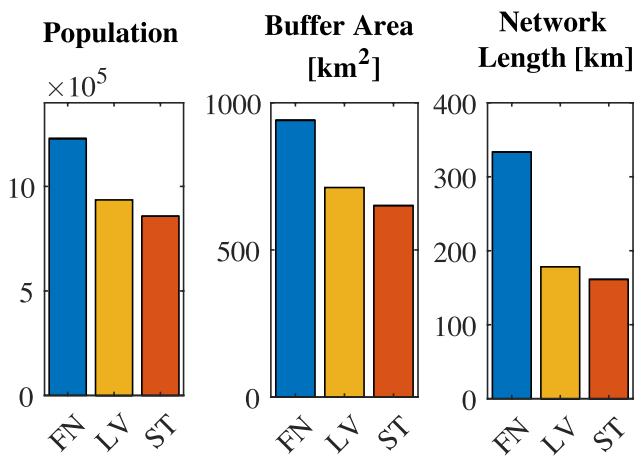

Figure 13. Indexes of population and area served by deployed networks. Metropolitan area of Atlanta.

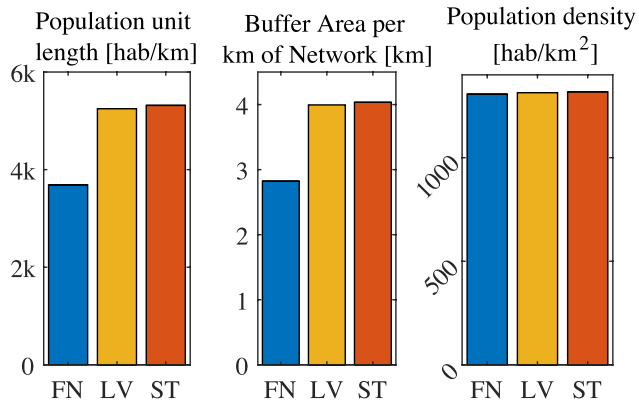

Figure 14. Normalized indexes of population and area served by deployed networks. Metropolitan area of Atlanta.

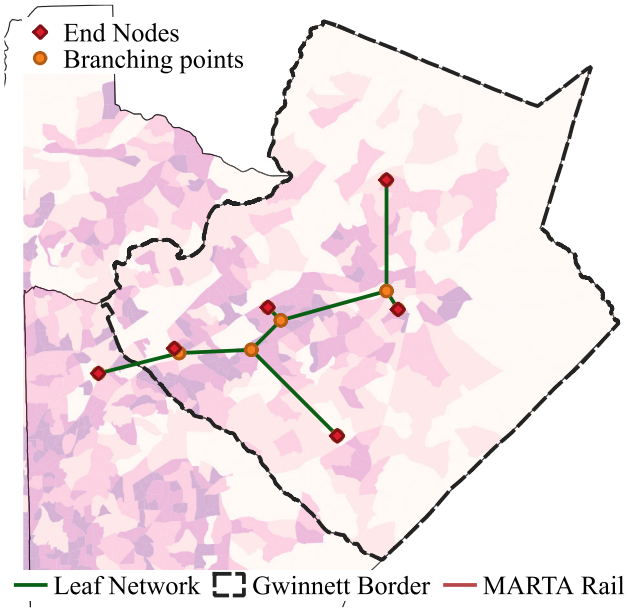

Figure 15. LV network deployed from the MARTA railway to five population centroids in Gwinnett county.

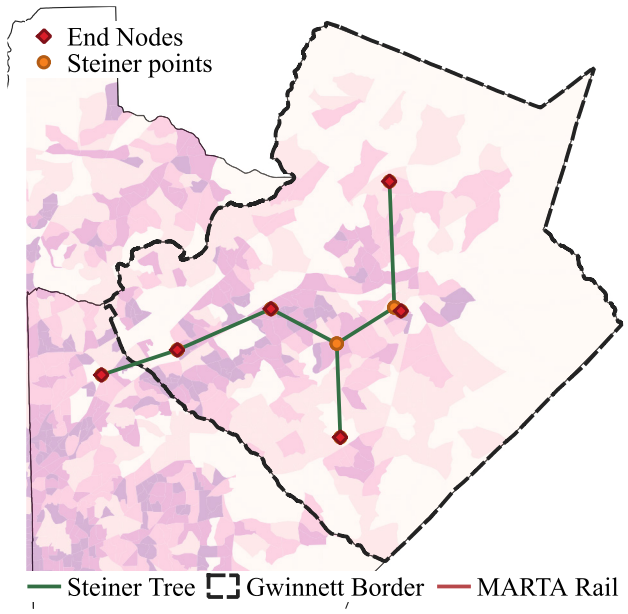

Figure 16. ST network deployed from the MARTA railway to five population centroids in Gwinnett County.

Table 2. Population and area reached by the LV and ST networks in Gwinnett County.

Network	Population per unit length [hab km^{-1}]	Area per unit length [km^2 m^{-1}]	Population Density [hab km^{-2}]
ST	4906.1	4.22	1160
LV	5086.6	4.15	1225

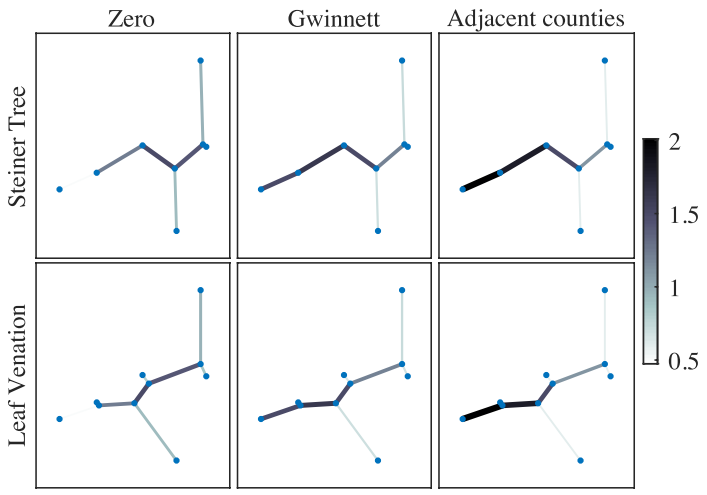

Figure 17. Traffic distribution as a function of source node weight for Gwinnett County. Edge thickness and intensity are proportional to their load.

STs are more cost efficient than LV networks. Nevertheless, as networks become more dependent on a source node, LV networks outperform STs, yielding a lower total cost even though the total network length is always higher than the ST. In the current example, both networks have the same cost when the weight of the source point corresponds to 0.64 times the county's population. Lastly, it is important to mention that regardless of the source node weight, the normalized cost per unit length of network is always lower for LV networks, and the difference increases with the dependency from the source node.

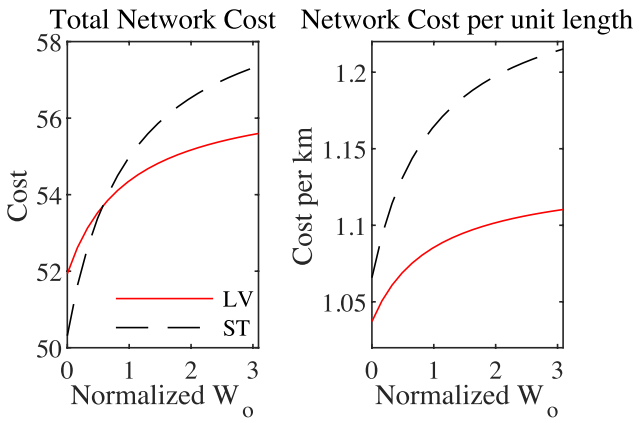

Figure 18. Total and unitary network cost as a function of source node weight—Gwinnett County.

5. Conclusion

Our simulation results show that the total length of LV networks is on average 10% larger than that of the minimum spanning tree (ST). Traffic distribution is slightly better in LVs than in STs, arguably because LVs have a larger total network length. Additionally, LVs exhibit higher efficiency building paths from the petiole (source node) to auxin points (attraction points) than between pairs of auxin points, which is consistent with the natural transport function of a leaf. These improvements on traffic distribution and path efficiency are achieved at the expense of an increase in total network length. This evolutionary trade-off can be studied using Pareto optimality in future studies.

The length of LV networks of uniform edge traffic capacity spanning from the center of the city of Atlanta towards a set of 15 population centroids around its metropolitan area was 10% higher than the theoretical minimum, with travel distances in average 16% higher than the Euclidean distance for paths connecting the source node to the attraction points (versus 32% for the ST). Distances between attraction nodes were in average 43% higher than the Euclidean distance (versus 45% for the ST). LV networks thus outperform STs for transportation to and from a central node, while keeping the total network length and travel distances close to the optimal solution. Additionally, LV networks are as efficient as ST in terms of area and population reached per unit of network length.

A simplified problem of railway expansion was solved with the LV and ST algorithms, in which the capacity of the edges was proportional to their construction cost. Both networks reached a similar population per unit of network length (3.5% more population with the LV than the ST). The relative weights of the population centroids highly influenced the distribution of edges thickness of the network. The traffic load was higher for edges adjacent to the source node at which the railroad expansion was initiated. The network cost per unit of network length was always lower for LVs than STs. The cost difference increased with the weight of the central (source) node. This means that even though LVs exhibit a higher network length, their total cost is lower than that of ST for centralized networks. This is an interesting result for the development of Atlanta, GA and for the enhancement of the transportation networks in many other cities in the world, like New-York (NY) or Paris (France).

We conclude that LV algorithms can efficiently assist the design of engineered transportation networks. Nevertheless, our study was restricted to transport optimization and actual engineering design must consider other constraints including interference with current infrastructure, construction methods and operation limitations. We propose that LV—inspired networks can be used to establish an initial design that can be refined based on environmental and engineering constraints. The advantage of using LV algorithms is that they achieve polynomial runtime instead of ST algorithms which are NP-complete. LVs are thus particularly suitable for determining initial network guesses that can then be iteratively optimized.

Conclusions of this study can be extended to multiple-connected networks in which secondary edges form loops. Network redundancy increases robustness at the expense of network cost. Additionally, LV algorithms can be used on continuous domains leveraging the assumption of discrete attraction points presented in this study. Lastly, there is an opportunity to expand LV algorithms to account for extra constraints; for instance, LV algorithms could be used to optimize routing or transport algorithms where the cost of the network is a complex function considering land cost, edge capacity and network tortuosity, rather than just a function of the network length.

Acknowledgments

This work was supported by the U.S National Science Foundation, under Grant CMMI#1552368: 'CAREER: Multiphysics Damage and Healing of

Rocks for Performance Enhancement of Geo-Storage Systems—A Bottom-Up Research and Education Approach'.

ORCID iDs

Fernando Patino-Ramirez https://orcid.org/0000-0003-1248-499X

References

[1] Sack L and Scoffoni C 2013 Leaf venation: structure, function, development, evolution, ecology and applications in the past, present and future *New Phytol.* **198** 983–1000
[2] Sanders H L and Wyatt S E 2009 Leaf evolution and development: advancing technologies, advancing understanding *Bioscience* **59** 17–26
[3] Kenrick P and Strullu-Derrien C 2014 The origin and early evolution of roots *Plant Phys.* **166** 570–80
[4] Kevin Boyce C 2005 The evolutionary history of roots and leaves *Vascular Transport in Plants* (New York: Elsevier) pp 479–99
[5] Whitney H 1931 A theorem on graphs *Ann. Math.* **32** 378
[6] Albert R, Jeong H and Barabási A L 2000 Error and attack tolerance of complex networks *Nature* **406** 378–82
[7] Barkai N and Leibler S 1997 Robustness in simple biochemical networks *Nature* **387** 913–7
[8] Aldana M and Cluzel P 2003 A natural class of robust networks *Proc. Natl Acad. Sci. USA* **100** 8710–4
[9] Draghi J A, Parsons T L, Wagner G P and Plotkin J B 2010 Mutational robustness can facilitate adaptation *Nature* **463** 353–5
[10] Gáspár M E and Csermely P 2012 Rigidity and flexibility of biological networks *Brief Funct. Genom.* **11** 443–56
[11] Udan R S, Culver J C and Dickinson M E 2013 Understanding vascular development *Wiley Interdiscip. Rev. Dev. Biol.* **2** 327–46
[12] Chandrasekhar A and Navlakha S 2019 Neural arbors are Pareto optimal *Proc. R. Soc.* B **286** 20182727
[13] Conn A, Pedmale U V, Chory J and Navlakha S 2017 High-resolution laser scanning reveals plant architectures that reflect universal network design principles *Cell Syst.* **5** 53–62.e3
[14] Hodge A, Berta G, Doussan C, Merchan F and Crespi M 2009 Plant root growth, architecture and function *Plant Soil* **321** 153–87
[15] Katuwal S, Vermang J, Cornelis W M, Gabriels D, Moldrup P and de Jonge L W 2013 Effect of root density on erosion and erodibility of a loamy soil under simulated rain *Soil Sci.* **178** 29–36
[16] Whalley W R, Leeds-Harrison P B, Leech P K, Riseley B and Bird N R A 2004 The hydraulic properties of soil at root-soil interface *Soil Sci.* **169** 90–9
[17] Yu H-W, Chen C-H and Lo W-C 2011 Mechanical behavior of the soil-root system *Soil Sci.* **176** 99–109
[18] Bebber D P, Hynes J, Darrah P R, Boddy L and Fricker M D 2007 Biological solutions to transport network design *Proc. R. Soc.* B **274** 2307–15
[19] Nakagaki T, Yamada H and Hara M 2004 Smart network solutions in an amoeboid organism *Biophys. Chem.* **107** 1–5
[20] Takamatsu A, Takaba E and Takizawa G 2009 Environment-dependent morphology in plasmodium of true slime mold *Physarum polycephalum* and a network growth model *J. Theor. Biol.* **256** 29–44
[21] Tero A, Nakagaki T, Toyabe K, Yumiki K and Kobayashi R 2010 A method inspired by *Physarum* for solving the Steiner problem *IJUC* **6** 109–23
[22] Tero A *et al* 2010 Rules for biologically inspired adaptive network design *Science* **327** 439–42
[23] Tero A, Kobayashi R and Nakagaki T 2006 Physarum solver: a biologically inspired method of road-network navigation *Physica* A **363** 115–9
[24] Tero A, Kobayashi R and Nakagaki T 2007 A mathematical model for adaptive transport network in path finding by true slime mold *J. Theor. Biol.* **244** 553–64
[25] Bottinelli A, van Wilgenburg E, Sumpter D J T and Latty T 2005 Local cost minimization in ant transport networks: from small-scale data to large-scale trade-offs *J. R. Soc. Interface* **12** 20150780
[26] Cabanes G, Van Wilgenburg E, Beekman M and Latty T 2015 Ants build transportation networks that optimize cost and efficiency at the expense of robustness *Behav. Ecol.* **26** 223–31
[27] van Wilgenburg E and Elgar M A 2007 Colony structure and spatial distribution of food resources in the polydomous meat ant *Iridomyrmex purpureus Insectes Soc.* **54** 5–10
[28] Perna A *et al* 2012 Individual rules for trail pattern formation in Argentine ants (*Linepithema humile*) *PLoS Comput. Biol.* **8** e1002592
[29] Buhl J *et al* 2004 Efficiency and robustness in ant networks of galleries *Eur. Phys. J.* B **42** 123–9
[30] Socha K and Dorigo M 2006 Ant colony optimization for continuous domains *Eur. J. Oper. Res.* **185** 758–62
[31] Perna A and Latty T 2014 Animal transportation networks *J. R. Soc. Interface* **11** 20140334
[32] Davies M S and Blackwell J 2007 Energy saving through trail following in a marine snail *Proc. R. Soc.* B **274** 1233–6
[33] Oka K, Aoyagi S, Arai Y, Isono Y, Hashiguchi G and Fujita H 2002 Fabrication of a micro needle for a trace blood test *Sensors Actuators* A **97–8** 478–85
[34] Fish F E, Weber P W, Murray M M and Howle L E 2011 The tubercles on humpback whales' flippers: application of bio-inspired technology *Integr. Comp. Biol.* **51** 203–13
[35] Ninan L, Monahan J, Stroshine R L, Wilker J J and Shi R 2003 Adhesive strength of marine mussel extracts on porcine skin *Biomaterials* **24** 4091–9
[36] Geem Z W 2009 Particle-swarm harmony search for water network design *Eng. Opt.* **41** 297–311
[37] Zhou H, Zhang Z, Wu Y and Qian T 2011 *Bio-Inspired Dynamic Composition and Reconfiguration of Service-Oriented Internetware Systems* (Berlin: Springer) pp 364–73
[38] Yang Z, Yu B and Cheng C 2007 A parallel ant colony algorithm for bus network optimization *Comput. Civ Infrastruct. Eng.* **22** 44–55
[39] Nelson T and Dengler N 1997 Leaf vascular pattern formation *Plant Cell.* **9** 1121–35
[40] Ronellenfitsch H and Katifori E 2016 Global optimization, local adaptation, and the role of growth in distribution networks *Phys. Rev. Lett.* **117** 1–5
[41] Katifori E, Szollosi G J and Magnasco M O 2010 Damage and fluctuations induce loops in optimal transport networks *Phys. Rev. Lett.* **104** 1–4
[42] Roth-Nebelsick A 2001 Evolution and function of leaf venation architecture: a review *Ann. Bot.* **87** 553–66
[43] Judd W S, Campbell C S, Kellogg E A, Stevens P F and Donoghue M J 2002 *Plant Systematics* (Massachusetts: Sinauer Sunderland)
[44] Runions A, Fuhrer M, Lane B, Federl P, Rolland-Lagan A-G and Prusinkiewicz P 2005 Modeling and visualization of leaf venation patterns *ACM Trans. Graph.* **24** 702
[45] Sachs T 1981 The control of the patterned differentiation of vascular tissues *Adv. Bot. Res.* **9** 151–262
[46] Aloni R, Schwalm K, Langhans M and Ullrich C I 2003 Gradual shifts in sites of free-auxin production during leaf-primordium development and their role in vascular differentiation and leaf morphogenesis in *Arabidopsis Planta* **216** 841–53
[47] Murray C D 1926 The physiological principle of minimum work: i. the vascular system and the cost of blood volume *Proc. Natl Acad. Sci. USA* **12** 207–14

[48] Teich J 2001 *Pareto-Front Exploration with Uncertain Objectives* (Berlin: Springer) pp 314–28
[49] Robins G and Zelikovsky A 2008 Minimum Steiner tree construction *Handb. Algorithms VLSI Phys. Autom.* ch 24 pp 487–508
[50] Wald J A and Colbourn C J 1983 Steiner trees in probabilistic networks *Microelectron. Reliab.* **23** 837–40
[51] Winter P and Zachariasen M 1997 Euclidean Steiner minimum trees: an improved exact algorithm *Networks* **30** 149–66
[52] Liu C-H, Yuan S-Y, Kuo S-Y and Chou Y-H 2009 An O(n log n) path-based obstacle-avoiding algorithm for rectilinear Steiner tree construction *46th ACM/IEEE Design Automation Conf.* pp 314–9
[53] Fampa M, Lee J and Maculan N 2016 An overview of exact algorithms for the euclidean Steiner tree problem in n-space *Int. Trans. Oper. Res.* **23** 861–74
[54] Ljubic I, Weiskircher R, Pferschy U, Klau G W, Mutzel P and Fischetti M 2006 An algorithm framework for the exact solution of the prize-collecting Steiner tree problem *Math. Program.* **105** 427–49
[55] Chow W K, Li L, Young E F Y and Sham C W 2014 Obstacle-avoiding rectilinear Steiner tree construction in sequential and parallel approach *Integr. VLSI J.* **47** 105–14
[56] Müller-Hannemann M and Tazari S 2010 A near linear time approximation scheme for Steiner tree among obstacles in the plane *Comput. Geom. Theor. Appl.* **43** 395–409
[57] Ajwani G, Chu C and Mak W K 2011 FOARS: FLUTE based obstacle-avoiding rectilinear Steiner tree construction *IEEE Trans. Comput. Des. Integr. Circuits Syst.* **30** 194–204
[58] Fonseca R, Brazil M, Winter P and Zachariasen M 2014 Faster exact algorithms for computing Steiner trees in higher dimensional euclidean spaces *11th DIMACS Implement Challenge Brown University*
[59] Suen J Y and Navlakha S 2019 Travel in city road networks follows similar transport trade-off principles to neural and plant arbors *J. R. Soc. Interface* **16** 154
[60] Blonder B, Wey T W, Dornhaus A, James R and Sih A 2012 Temporal dynamics and network analysis *Methods Ecol Evol.* **3** 958–72
[61] Willebeek-LeMair M H and Reeves A P 1993 Strategies for dynamic load balancing on highly parallel computers *IEEE Trans. Parallel Distrib. Syst.* **4** 979–93
[62] Barthelemy M 2004 Betweenness centrality in large complex networks *Eur. Phys. J.* B **38** 163–8
[63] Newman M E J 2005 A measure of betweenness centrality based on random walks *Soc. Netw.* **27** 39–54
[64] Biba S, Curtin K M and Manca G 2010 A new method for determining the population with walking access to transit *Int. J. Geogr. Inf. Sci.* **24** 347–64
[65] O'Sullivan D, Morrison A and Shearer J 2000 Using desktop GIS for the investigation of accessibility by public transport: an isochrone approach *Int. J. Geogr. Inf. Sci.* **14** 85–104